frontiers | Frontiers in Marine Science

TYPE Original Research
PUBLISHED 19 November 2024
DOI 10.3389/fmars.2024.1492115

OPEN ACCESS

EDITED BY
Carlos Moreno,
University of Cádiz, Spain

REVIEWED BY
Dawei Pan,
Chinese Academy of Sciences (CAS), China
Miguel Oliver Rodríguez,
University of the Balearic Islands, Spain

*CORRESPONDENCE
Xiangfeng Kong
kxf_1985@163.com
Nan Gao
nangao@qlu.edu.cn

RECEIVED 06 September 2024
ACCEPTED 30 October 2024
PUBLISHED 19 November 2024

CITATION
Zhang Y, Chen S, Liu Y, Zou Y, Wang Y, Zhang S, Kong X, Gao Y and Gao N (2024) Automatic *in situ* sensor based on $K_2S_2O_8$ oxidation method for total phosphorus detection in marine water. *Front. Mar. Sci.* 11:1492115. doi: 10.3389/fmars.2024.1492115

Automatic *in situ* sensor based on $K_2S_2O_8$ oxidation method for total phosphorus detection in marine water

Yanmin Zhang[1,2], Shougang Chen[1], Yan Liu[2,3], Yan Zou[2,3], Yang Wang[2,3], Shuwei Zhang[2,3], Xiangfeng Kong[2,3]*, Yang Gao[2,3] and Nan Gao[2,3]*

[1]Department of Materials Science and Engineering, Ocean University of China, Qingdao, China, [2]Institute of Oceanographic Instrumentation, Qilu University of Technology (Shandong Academy of Sciences), Qingdao, China, [3]Laoshan Laboratory, Qingdao, China

Phosphorus is a key indicator for water quality management due to its role in eutrophication. The variety of phosphorus-containing substances necessitates highly sensitive detection of total phosphorus, particularly through automated methods, to ensure water safety. This study involved the independent development of a sensor featuring an automated *in situ* detection technique. Utilizing potassium persulfate high-temperature oxidation and phosphorus molybdenum blue spectrophotometry, total phosphorus was monitored *in situ* via sequential injection technology. Additionally, the detection process and reaction conditions of the sensor were optimized, and a temperature compensation algorithm and turbidity correction were applied to mitigate environmental factors. Under optimal conditions, the sensor demonstrated a detection limit of 1.9 μg/L with a range of 6.5–1000 μg/L in seawater, and 1.2 μg/L with a range of 4.1–2000 μg/L in freshwater. The digestion efficiency for five representative phosphorus-containing substances was found to range from 87.3% ± 1.7% to 103.1% ± 0.6%. Notably, the sensor was deployed for *in situ* operation at a marine experimental station and online at a river monitoring station. With its integration, low power consumption, and high precision, the sensor enabled long-term unattended monitoring, delivering accurate, stable, and reliable results.

KEYWORDS

total phosphorus, *in situ* sensor, sequential injection analysis, water samples, temperature compensation

1 Introduction

Phosphorus, a critical nutrient for the growth of all life forms, is typically regarded as the limiting factor for primary productivity in lakes and oceans (Rusakov et al., 2022). In aquatic environments, phosphorus can be present in several forms, including elemental phosphorus, orthophosphate, condensed phosphate, pyrophosphate, metaphosphate, and

phosphate bound to organic groups. Therefore, total phosphorus (TP) represents the aggregate of all these phosphorus species. Excessive phosphorus in water promotes the growth of aquatic plants, leading to algal blooms and eutrophication (Mahmud et al., 2020). Consequently, accurate detection of total phosphorus is essential for assessing phosphorus levels and ensuring water safety.

Currently, ion chromatography (Yokoyama et al., 2009), fluorescence (Zhao et al., 2011) and UV-Vis absorbance (Shyla et al., 2011) are widely employed for quantitative phosphorus detection (Alam et al., 2021; Jia et al., 2023). Nevertheless, chromatography and fluorescence methods are infrequently used due to their high cost and time demands (Wu et al., 2022). UV-Vis absorbance spectrophotometry is the most prevalent detection method, with molybdate spectrophotometry being a standard approach for determining TP concentrations. These techniques necessitate field sampling and pretreatment prior to laboratory analysis, resulting in significant time delays, labor intensity, and high costs, which are insufficient for modern detection management. Moreover, water samples may be subjected to stimuli and contamination during transportation, potentially impacting the accuracy of the detection results. Therefore, it is imperative to develop instruments for automatic detection techniques for determining the TP concentration because of the minimum number of random errors, high degree of repetition, and low degree of sample handling in the automated operation mode.

In recent years, considerable research has been conducted on automatic monitoring instruments to reduce manual labor and streamline detection procedures. These studies have focused on two main categories: online monitoring and *in-situ* analysis equipment (Liu et al., 2016; Lin et al., 2017; MaChado et al., 2017; Zhang et al., 2019; Yasui-Tamura et al., 2020; Lin et al., 2021). Notably, *in situ* analysis allows for the examination of samples at their original location, providing real-time and accurate measurements of sample concentration changes. Consequently, *in situ* analytical instruments have become increasingly necessary and have garnered significant attention (Nightingale et al., 2015; Liu et al., 2016; Lin et al., 2017; MaChado et al., 2017; Zhang et al., 2019).

Analytical methods suitable for *in situ* measurements of TP exhibit various limitations regarding speed and permissible uncertainties, with precision and sensitivity influenced by potential interferences and applicability (Yokoyama et al., 2009). Flow analysis technology, encompassing flow injection analysis (FIA), sequential injection analysis(SIA), segmented continuous flow analysis(SCFA), and loop flow analysis(LFA), has demonstrated significant utility in enhancing sensitivity within automatic monitoring instruments (Zhao et al., 2011; Nightingale et al., 2015; Dafner, 2016; Wu et al., 2022; Ruzicka and Chocholou, 2024). For instance, Yang et al. reviewed different injection techniques and evaluated the advantages and drawbacks of various methods (Yang et al., 2019). Among the automatic injection techniques, FIA is frequently employed. Due to the use of peristaltic pumps in FIA, the system operates under continuous flow conditions and can achieve high sample throughput, but at the cost of higher reagent usage (Worsfold et al., 2013). SIA, as the second generation method of FIA, is a fully automated flow analysis technology that serves as a more environmentally friendly alternative, where the suction and distribution of liquids are completely computer-controlled. SIA utilizes the principle of multi directional switching, using a multi port selector valve and a reversible pump, which can modify the fluid dynamics conditions by simply changing the programming of the valve and pump (Biocic et al., 2024, 2024). In addition, as a fully computer-controlled technology, SIA not only minimizes errors in manual detection, precisely controls the amount of as-used samples and reagents, reduces the generation of waste and the consumption of solution, but also has higher accuracy and repeatability in detection results (Al-Shwaiyat et al., 2024; Tambaru et al., 2024). Because of these advantages, combining the SIA technique with UV-vis absorption spectrophotometry turn into the most available technique in analytical laboratories, which allows for automation, miniaturization and rapid analysis.

In the past five years, a large amount of literature and articles on the application of flow analysis technology in water environment monitoring has been reported. There are already many *in situ* sensors, including nitrate and nitrite (Yang et al., 2019; Liu et al., 2024), total alkalinity (Sonnichsen et al., 2023), pH (Perez de Vargas Sansalvador et al., 2016; Yin et al., 2021), iron (Geißler et al., 2017), manganese (Geißler et al., 2021) and so on. Phosphate *in situ* sensors have also been reported (Yang et al., 2020; Morgan et al., 2021), but total phosphorus *in situ* sensors based on the SIA method are rarely reported, even though there are many theoretical studies on the field monitoring of TP in seawater.

In this study, an automatic *in-situ* sensor for detecting TP in water was developed based on the principles of potassium persulfate oxidation and phosphorus molybdenum blue with sequential injection analysis. To enhance analytical performance and expedite the detection process, the detection scheme was progressively optimized through detailed research on digestion time, temperature, oxidant concentration, phosphomolybdic blue coloring time, and reagent stability over time. Watertightness and impact vibration tests were conducted to assess the seaworthiness of the instrument, ensuring its capability to perform *in situ* sample measurements underwater. Additionally, a temperature compensation algorithm was optimized to more accurately reflect the total phosphorus concentration relative to water quality. The *in situ* sensor was deployed at Zhongyuan dock, with an overall monitoring cycle of one month due to limited chemical reagent usage. During the demonstration period, regular manual sampling and laboratory testing were performed, and the results were compared with those from the *in situ* sensors. The findings indicated that the developed *in situ* TP sensor successfully enables monitoring of TP concentration in water.

2 Materials and methods

2.1 Materials

All chemicals were sourced from Sigma-Aldrich and included analytical grade chemicals, potassium persulfate (PDS), boric acid

(H_3BO_3), sodium molybdate(Na_2MoO_4), potassium antimony(III) tartrate hydrate ($C_8H_4K_2O_{12}Sb_2{\cdot}_3H_2O$), sulfuric acid solution (H_2SO_4), ascorbic acid($C_6H_8O_6$), sodium chloride(NaCl), magnesium sulfate($MgSO_4$) and sodium bicarbonate($NaHCO_3$), β-sodium glycerophosphate($C_3H_{12}NaO_7P$, β-SGP); 5-pyridoxal phosphate monohydrate ($C_8H_{10}NO_6P$, 5-PP); sodium hexametaphosphate($(NaPO_3)_6$, SHP); sodium pyrophosphate ($Na_4P_2O_7$, SPP); and adenosine 5'-triphosphate($C_{10}H_{16}N_5O_{13}P_3$, ATP) were used as received without further purification. Potassium dihydrogen phosphate (KH_2PO_4) was oven-dried at 100°C for 1 h prior to use, while other chemicals were utilized as received. All solutions were prepared using freshly made ultrapure water (resistivity≥18.2MΩ cm) from a Millipore water purification system (Millipore Co., USA).

Artificial seawater was utilized as the solvent for the preparation of standard solutions instead of DI water. Artificial seawater was first prepared by dissolving 31 g of sodium chloride, 10 g of magnesium sulfate, and 0.05 g of sodium bicarbonate in 1 L of DI water. Subsequently, a standard solution of TP was prepared by dissolving 0.1614 g of β-SGP in 1 L of artificial seawater. A standard phosphate solution was obtained by dissolving 0.4390 g of potassium dihydrogen phosphate in 1 L of artificial seawater.

The oxidation reagent was prepared as follows: 6.0 g of potassium persulfate and 3.6 g of boric acid were dissolved in 150 mL of DI water by continuous stirring for 5 min, after which the solution volume was adjusted to 200 mL in a volumetric flask.

Preparation of Molybdate Solution (MS): To prepare this solution, 0.0960 g of $C_8H_4K_2O_{12}Sb_2{\cdot}_3H_2O$ and 4.44 g of Na_2MoO_4 were completely dissolved in 100 mL of deionized water to yield a clear solution. Subsequently, 100 mL of 20% (concentration fraction) sulfuric acid was gradually added to this mixture. The final volume of the prepared solution was adjusted to 200 mL. The solution, which has a validity period of six months, was then transferred to a plastic bottle for future use.

Preparation of ascorbic acid solution (Vc): For this, 10.8 g of ascorbic acid was dissolved in 200 mL of deionized water. The resulting colorless solution was stored at 5°C and remained effective for one month.

2.2 Analytical system design

In this study, the automatic *in situ* sensor employed the SIA method, akin to the previously described total nitrogen analysis (Zhang et al., 2020). Figure 1A illustrates an internal schematic diagram of the *in situ* sensor for total phosphorus. The method involves oxidizing all phosphorus forms to orthophosphate and detecting the total orthophosphate using a colorimetric assay. Several oxidation techniques have been utilized for converting organic phosphorus to phosphate, including sulfuric acid-nitric acid digestion, dry ashing, microwave digestion, potassium persulfate thermal digestion, UV-based oxidation, Fenton–Fenton-like reaction, and electrochemical oxidation (Rott et al., 2017; Sun et al., 2019; Gray et al., 2020; Lei et al., 2020; Zhu et al., 2021; Sun et al., 2022). Among these methods, high-temperature digestion is favored due to its use of mild chemicals with low toxicity, reduced reagent consumption, and rapid reaction speed, making it a classic and effective technique (Zhao et al., 2021). A fully integrated analytical system was thus developed, combining thermal digestion and colorimetric determination for the precise quantification of TP.

The sensor's appearance is depicted in Figure 1B; it measures 50 cm in height, 20 cm in diameter, and weighs 15 kg, including all reagents. The sensor has undergone water tightness treatment,

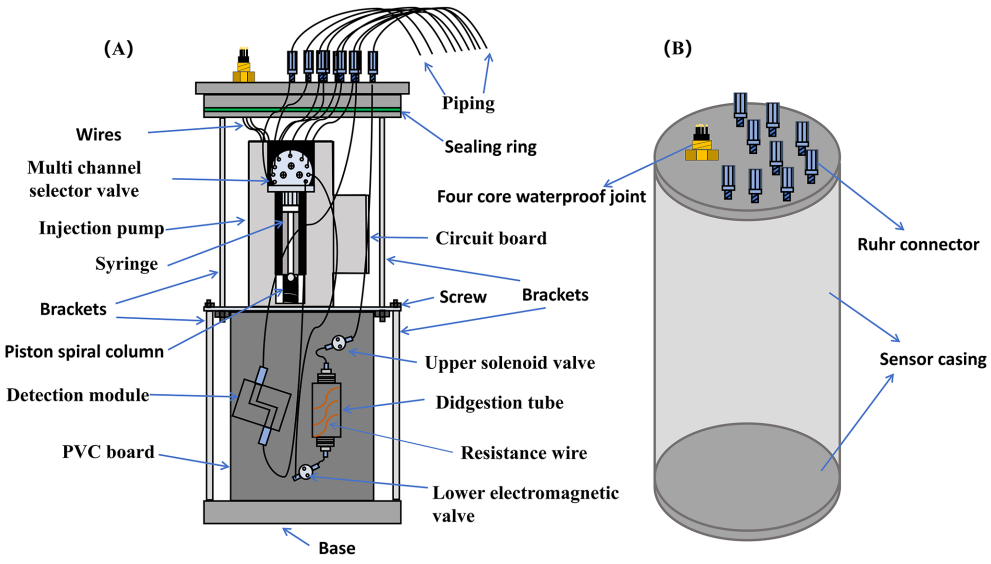

FIGURE 1
Internal and external design drawings of the sensor. **(A)** The design schematic of the TP analytical system; **(B)** The appearance of sensor. The blue small piece at the connection between the pipeline and sensor components represents the Ruhr connector. One end of the wire is connected to a waterproof joint, and the other end is partially connected to an injection pump for power supply and control of pump operation; Part of it is connected to the circuit board to ensure the normal operation and communication of the sensor.

where sealing rings are placed at the connections between the sensor housing, pipelines, and cables to meet its requirements for underwater operation. Besides, a sealing ring is placed at the connection between the sensor cover and the outer cylinder and coated with silicone grease to ensure the water tightness of the sensor. Prior to *in situ* testing, the sealing and pressure tests are conducted to ensure that the sensor could meet the requirements of 0-10m underwater measurements. During underwater operation, the sensor is powered by an onshore power source. Electricity and communication are connected to the water tight port on the top of the analyzer through a water tight cable. The sensor's average power consumption is about 10 W. A separate electronic-chemical structure was incorporated into the design to safeguard the electronic components from exposure to wet chemicals. Consequently, the *in situ* sensor mainly contents the circuit board, syringe pump (Cavro® XCalibur Modular Digital Pump, 733085-B), and multichannel selection valve (Tecan Cavro 9-port selector ceramic valve, 1/4-28 XC) which are the core of the sensor; the digestion module and the detection module (Figure 1A).

In addition, we also independently designed and developed the sensor operation software. The software structure is mainly divided into two parts, namely, the parameter setting function and the operation control function. The parameter setting function is mainly designed for the debugging and calibration of the instrument, paying more attention to the detailed parameter adjustment and result feedback calibration during the instrument work, and providing more functional support for technical support personnel. The operation control function mainly controls the operation process of the instrument, and measures total phosphorus, mainly designed for users. The software communicates with the total phosphorus sensor through the RS485 interface. The description of sensor operation software is shown in Table 1.

The syringe pump was combined with multichannel selection valves to automate the injection and flow for the chemical reaction. A 9-channel valve equipped with 1.5 mm/2.5 mm i.d. PTFE tubing (BE-FLUIDICS, Shanghai) was used to deliver the reagent and sample to the corresponding positions for chemical reactions. After the reaction, these samples were transferred to the detection module to complete the *in situ* detection of TP. Typically, a holding coil is included in the SIA system where the sample and reagents can be collected, preventing contamination of the syringe. In this work, the typical sequential injection method is improved by directly connecting the injector to the multi-channel selector valve. To avoid cross contamination, we have added a cleaning process and set the pump speed of the injection pump to the highest value during cleaning. The rapid cleaning of the syringe was shorter than 1 min, with the faster flushing, resulting in greater cleaning force and better effectiveness. In addition, the flow path in this sensor has been simplified.

The digestion process involves the conversion of phosphorus substances and persulfate into orthophosphate under acidic

TABLE 1 Description of sensor operation software.

	Function	Parameter Declaration
Operation control	standard curve	$y=Ax^2+Bx+C$; A: +0001.23;B: +0002.34; C: +0003.45
	Pump initialization	Syringe returns to zero position
	Pump open	Turn on the pump
	Pump off	Turn off the pump
	Fill	Filling of reagents
	Sample injection	Sample tube injection
	Wash 1	Clean all pipelines before sample testing, evacuate the pure water in the digestion tube, and clean the pipelines once with both sample and pure water
	Wash 2	Clean after sample testing, clean all pipelines with pure water after each sample testing, and finally fill the digestion tube and detection tank with pure water
	Single run	the entire process of sample testing, namely: cleaning 1- reagent filling - injection - digestion - detection - cleaning 2
	Automatic operation	can set the number of automatic runs and interval time, used for *in-situ* testing or multiple laboratory sample testing. Scheduled automatic operation, the number of runs cannot be 0, and if the number of digits is insufficient, use 0 to make up for it
	System reset	All parameters are powered off and retained
Parameter settings	Read EEPROM storage data	Read standard curve, digestion time, digestion temperature setting parameters
	Digestion time	Digestion time, 0 - xxx min
	Diestion temperature	Diestion temperature, 0 - xxx °C
	Color development time	Phosphorus molybdenum blue reaction time setting, 0 - xx min

conditions through a high-temperature digestion reaction. The digestion module suitable for high temperature and high pressure conditions consists of a cylindrical quartz glass tube with both upper and lower openings, onto which a 12 cm long φ0.45 mm resistance wire is wound (Figure 1A). The resistance wire heats the liquid in the digestion tube, and a temperature probe is installed to regulate the digestion temperature. The inlet and outlet of the digestion tube are connected to two solenoid valves (Shanghai Leqi Fluid, HV-12516), which should be closed during digestion to maintain a sealed state and prevent liquid splashing at high temperatures. The sample and digestion reagents are delivered to the digestion tube via the injection pump and selection valve, and mixing is facilitated by injecting bubbles into the digestion tube. Afterwards, the resistance wire is powered for heating. When the temperature reaches 120°C, the resistance wire power supply is disconnected. When the temperature drops below 120°C, heating continues to ensure that the temperature remains at 120°C during the digestion time. The digestion tube is made of quartz material and has undergone long-term experiments to meet the requirements of current instrument equipment, which adopts commonly used components for total nitrogen analyzer, total phosphorus analyzer, and chemical oxygen demand (COD) analyzer in environmental protection systems. In this system, the digestion tube has also been sealed with sealing rings placed at the pipeline joints. During the experiment, it was found that the liquid would boil during the digestion process by the digestion tube leaked air, posing a risk of operation. Therefore, we also conducted experiments to ensure good sealing of the digestion tube after installation.

The detection module comprises a customized Z-type flow cell (3.0 cm path length, 1.5 mL volume), an 880 nm central wavelength LED lamp equipped with a beam splitter, and a photodiode. The emission spectra of the LED and the absorption spectra of the products formed by the PMB reaction are well-aligned, enabling accurate determination of the relationship between phosphate concentration and absorbance. The inclusion of a beam splitter enhances detection performance by reducing the detection limit.

2.3 Experimental process

The principle of TP detection is to first convert organic and inorganic phosphorus to orthophosphate and then perform colorimetric measurements on the orthophosphate. The steps of single measurements of TP is shown in Table 2. In a typical experiment, a 1930 μL sample and 70 μL oxidant were drawn through a syringe and injected into the digestion tube in sequence. The solenoid valves at both ends were closed, the samples were heated, and the temperature was maintained for 20 min after it rose to 120°C. The TP samples were oxidized by potassium persulfate. In

TABLE 2 The SIA steps of the TP determination.

Process	Operation steps	Volume μL	Speed μL/s	Valve position
	Pump initialization	/	/	/
Clean the digestion tube and evacuate it	Open the solenoid valve	/	/	/
	Extract the solution from the digestion tube	2500	500	8
	Syringe emptying	2500	500	9
	Sample filling syringe	2000	500	3
	Empty the syringe	2000	500	9
	Sample filling syringe	2000	500	3
	Empty the syringe	2000	500	9
Sample mixing, digestion	Sample injection	1930	300	3
	Injecting oxidant	70	300	4
	Inject the mixed solution into the digestion tube	2000	300	8
	Extract the solution from the digestion tube	2200	300	8
	Inject the mixed solution into the digestion tube	2200	300	8
	Injector sucks air	100	300	5
	Inject into the digestion tube	100	300	8
	Close the solenoid valve	/	/	/
	Start heating up, maintain the temperature at 120°C, digest for 20 minutes, cool down for 5 minutes, and then open the solenoid valve	/	/	/
Clean the syringe	Sample filling syringe	2000	500	3

(Continued)

10.3389/fmars.2024.1492115

TABLE 2 Continued

Process	Operation steps	Volume μL	Speed μL/s	Valve position
	Empty the syringe	2000	500	9
	Pure water filled syringe	2000	500	1
	Empty the syringe	2000	500	9
Reagent mixing leads to color reaction	Ms injection	300	300	6
	VC injection	83	300	7
	Extract the solution from the digestion tube	2000	300	8
	Inject into the digestion tube	2383	300	8
	Injector sucks air	200	300	5
	Inject into the digestion tube	200	300	8
Clean the injector and inspect the pipeline	Sample filling syringe	2000	500	3
	Empty the syringe	2000	500	9
	Sample filling syringe	2000	500	3
	Empty the syringe	2000	500	9
	Sample filling syringe	2000	500	3
	Empty the syringe	2000	300	9
Test the blank absorbance of the sample	Open the detection module	/	/	/
	Detect absorbance	/	/	/
Clean the injector and inspect the pipeline	Pure water filled syringe	2000	500	1
	Empty the syringe	2000	500	9
Detect the absorbance of phosphomolybdic blue reaction	Extract the solution from the digestion tube	2500	500	8
	Empty the syringe	2500	300	9
	Measure absorbance and calculate concentration	/	/	/
Clean the injector and inspect the pipeline	Sample filling syringe	2000	500	3
	Empty the syringe	2000	500	9
	Pure water filled syringe	2000	500	1
	Empty the syringe	2000	500	9
Clean and fill the digestion tube	Pure water filled syringe	2000	500	1
	Inject into the digestion tank	2000	500	8
	Pure water filled syringe	2000	500	1
	Empty the syringe	2000	500	9
Clean and fill the detection pipeline	Pure water filled syringe	2000	500	1
	Empty the syringe	2000	500	9

order to reduce power consumption, the natural cooling was chosen in the digestion module instead of an exhaust fan. According to our previous experience, the sensor cooling can be reduced to below 90 degrees for about 5min, and it is safe to open the solenoid valve at this temperature. Potassium persulfate has a symmetrical structure with a bond energy of 140 kJ/mol, and the O-O bond distance is 1.497 Å (Zhao et al., 2013). The essential mechanism of potassium persulfate activation is O-O bond cleavage. The energy input at high temperatures (>60°C) can cause the fission of O-O bonds to form sulfate radicals, as shown in Equation 1:

$$S_2O_8^{2-} \rightarrow 2SO_4^{\bullet -} \quad (1)$$

Hydroxyl radicals were the predominant radicals generated during the heat activation of the persulfate process (Zhu et al., 2021), suggesting that sulfate radicals rapidly converted into hydroxyl radicals during the heating process, as illustrated in

Equation 2 (Matzek and Carter, 2016).

$$SO_4^{\bullet -} + H_2O \rightarrow SO_4^{2-} + HO^{\bullet} + H^+ \quad (2)$$

In most reaction systems, the reaction between sulfate radicals and water is too slow to be significant, with a reaction rate of Equation 2 being very low ($< 2 \times 10^{-3}$ s^{-1}) (Zhao et al., 2021). However, high temperatures can considerably accelerate this reaction rate. At specific temperatures, pH also influences the conversion of sulfate radicals to hydroxyl radicals. It has been reported that $SO4^{\bullet -}$ is the predominant radical at pH< 7; both $SO4^{\bullet -}$ and $HO^{\bullet}$ are present at pH = 9, and $HO^{\bullet}$ is the predominant radical at pH = 12 (Yang et al., 2010).

OH• is the neutral form of hydroxide ions, representing hydroxyl radicals, (OH^-). Hydroxyl radicals are highly reactive and function as strong oxidizers (Wang and Wang, 2018; Zhao et al., 2021). In this work, sulfate radicals were employed to oxidize the phosphorus to orthophosphate.

After digestion, the solenoid valves at both ends were then opened following a 5-min cooling Period (temperature among 80-90°C). Inject the MS and Vc into the digestion tube separately, mix evenly, and complete the phosphomolybdenum blue (PMB) color reaction of orthophosphate. After completing the filtered sample absorbance detection, inject the colorimetric solution from the digestion tube into the detection cell for absorbance detection (Figure 2A). The pipeline connection is shown in Figure 2B. Absorbance was measured at the maximum wavelength of 880 nm. In brief, the syringe extracts 300 μL of MS and 83.33 μL of Vc, which are injected into the digestion tube and mixed by moving the syringe back and forth to ensure thorough mixing. The syringe then removes 2 mL of the sample from the sample port and transfers it to the detection tank. These steps are repeated three times. The first two steps involve cleaning the syringe, while the final step measures the blank absorbance of the sample to account for turbidity. During the third run, the LED lamp (center wavelength 880 nm) is activated, and the optical signal is converted into an electrical signal by the photodiode; the signal value of the sample is recorded as I_0. Subsequently, the PMB solution is injected into the detection cell. After 30 s, the solution's color development is complete, and the light intensity I_1 is recorded. The absorbance of the solution is calculated using the formula $A = \lg (I_1/I_0)$, and the concentration of the sample is determined using the linear relationship between absorbance and the standard solution. The reaction principles of phosphomolybdenum blue are shown in Formulas 3 and 4.

$$PO_4^{3-} + 12MoO_4^{2-} + 27H^+ \rightarrow H_3PO_4(MoO_3)_{12} + 12H_2O \quad (3)$$

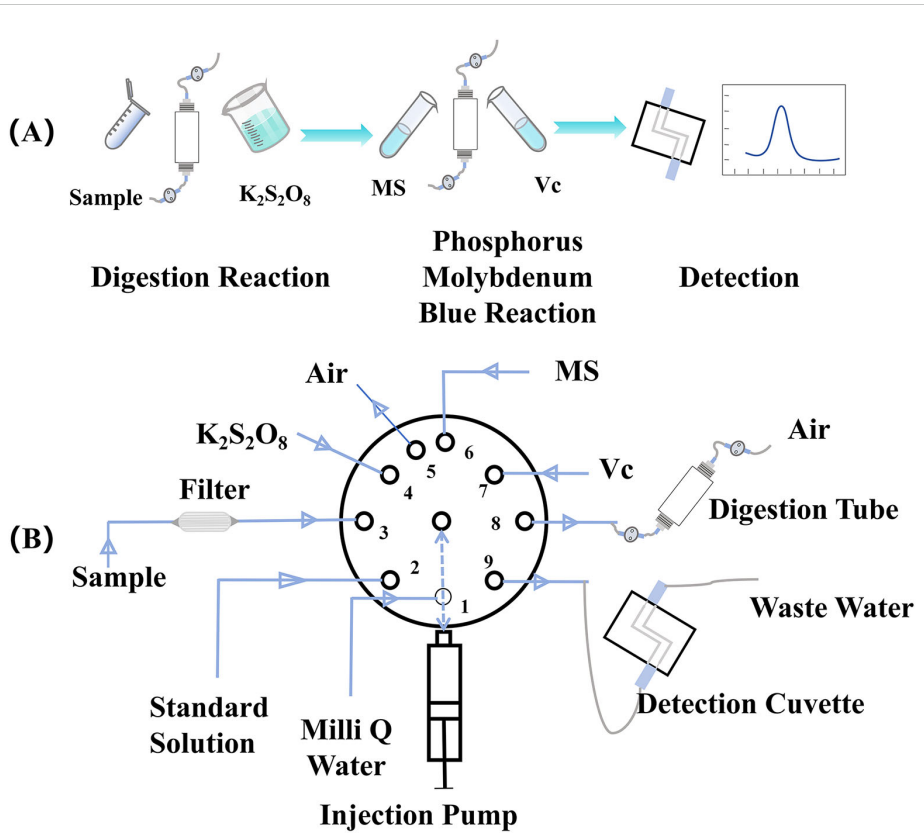

FIGURE 2
The reaction flowchart. **(A)** was the reaction process diagram and **(B)** was the diagram of pipeline connection, where the MS represents molybdate solution, Vc represents ascorbic acid solution. The number on the selection valve represents the channel, where 1 connecting DI water; 2 connects the standard solution; 3 is the injection channel, the sample through the filter after the connection of the valve port; 4 connects the oxidant; 5 connects air; 6 connects MS; 7 connects Vc; 8 connects the digestion pool; 9 connects the detection pool, and waste liquid also flows through the valve port.

$$H_3PO_4(MoO_3)_{12} + \text{Redutant} \rightarrow [H_4PMo(VI)_8Mo(V)_4O_{40}]^{3-} \quad (4)$$

2.4 Sensor characterization

The performance of the sensor is primarily indicated by parameters including accuracy, precision, linearity, and the lower detection limit. The specific parameters and calculation methods are listed in the supplementary document.

2.5 Practical application demonstration

Following the evaluation of the automatic *in situ* sensor's performance, a series of engineering tests were conducted, including vibration shock, high- and low-temperature, and salt spray experiments, to further assess its suitability for real marine environments.

Subsequently, *in situ* experiments were performed at the Qingdao wharf barge to monitor changes in total phosphorus concentration in seawater. The sensor operated five times daily. During this period, water samples were collected two days a month near the sensors for laboratory analysis, and the results were compared with those obtained from the sensor.

For comparison purposes, samples from near the sensor location were collected immediately, stored in plastic bottles at 4°C, and analyzed in the laboratory within one week of collection.

2.6 Statistical analysis

The research data is analyzed using Origin 2019b software (OriginLab, USA).

3 Results and discussion

3.1 Optimization of reagent concentrations

The efficiency of digestion is critical for accurate total phosphorus monitoring. To improve oxidation efficiency and reduce the detection limit, optimization of the oxidation reaction parameters—such as oxidizer concentration, pH, oxidation time, and reaction temperature—is required. A 1.00 mg/L sodium β-glycerophosphate solution (calculated by P) was used to evaluate oxidation efficiency under varying oxidizer concentrations and reaction conditions. The correlation between absorbance and potassium persulfate concentration was examined within the range of 25 to 35 mg/L. As shown in Figure 3A, the optimal oxidation rate was achieved at a concentration of 30 mg/L. Research indicates that insufficient oxidants are provided by low persulfate concentrations, while high persulfate concentrations hinder the reaction rate. Increased persulfate content in the digestion solution notably lengthened the time needed for complete color development during the phosphate measurement process; however, it did not affect the maximum absorbance of phosphoantimonylmolybdenum at 880 nm within the adequate color development period. Thus, the absorbance of samples digested with higher persulfate concentrations was lower, given the same digestion and color development durations.

According to reactions (1) and (2), hydroxyl radicals ($OH^{\bullet}$), generated from water molecules (H_2O) and persulfate ($S_2O_8^{2-}$), influence the efficiency of phosphorus oxidation. Therefore, it is essential to control the optimal pH and persulfate concentration to ensure sufficient OH• for the oxidation of total phosphorus. H_3BO_3 was employed as a pH regulator to investigate changes in absorbance with varying concentrations from 12 g/L to 20 g/L (Figure 3B). As depicted in Figure 3B, the absorbance peaked at 1.13 when the concentration of H_3BO_3 was 18 g/L, and decreased at both lower and higher concentrations. Thus, the optimal concentration for the reaction was determined to be 18 g/L H_3BO_3.

Several methods are available for digesting total phosphorus with potassium persulfate, with high-temperature and high-pressure digestion being the most commonly used. The thermal decomposition of persulfate between 50°C and 130°C adheres to an Arrhenius relationship, with a half-life of about 30 s at 130°C and 4 h at 75°C (Peyton, 1993; Doyle et al., 2004). A range of temperatures from 110°C to 130°C was examined using this potassium persulfate-thermal method. The results indicated that the optimal reaction temperature was 120°C, which remained relatively stable at around 0.97°C (Figure 3C).

Figure 3D illustrates the digestion efficiency for various oxidation times. The optimal oxidation time was determined to be 20 min, with an absorbance value of 0.97. Shorter oxidation times lead to insufficient oxidation of phosphorus in the solution and incomplete conversion to orthophosphate, resulting in incomplete oxidation reactions. Conversely, extending the reaction time to 30 min causes significant evaporation of the sample solution, reducing the absorbance to 0.92. Therefore, the following conditions were established for subsequent experiments: oxidizer (30 g/L potassium persulfate), pH (18 g/L H_3BO_3), temperature (120°C), and oxidation time (20 min).

Following phosphorus digestion, both organic and inorganic phosphorus are converted into orthophosphate, which remains as the final form of phosphorus. Spectrophotometry is widely utilized for phosphate analysis, despite growing interest in nanomaterial-based colorimetric sensors in recent years. The PMB method remains the most commonly employed technique (Li et al., 2019; Pinyorospathum et al., 2019; Salem and Draz, 2020). This chemical process begins with the reaction of orthophosphate with acidic molybdate to produce 12-molybdophosphoric acid, which is then reduced to PMB, as described in Equations 3 and 4 (Nagul et al., 2015). The concentration of total phosphorus is calculated based on the relationship between the absorbance at 880 nm and the concentration of PMB.

Different reagent concentrations were examined to determine the optimal color reaction. Based on a univariate experimental design, the reagent concentration for comparative color analysis was refined. The optimal injection volume for the sodium molybdate mixture was found to be 300 μL, with both higher and lower volumes resulting in reduced absorbance values (Figure 4A). Figure 4B illustrates the change in absorbance with increasing

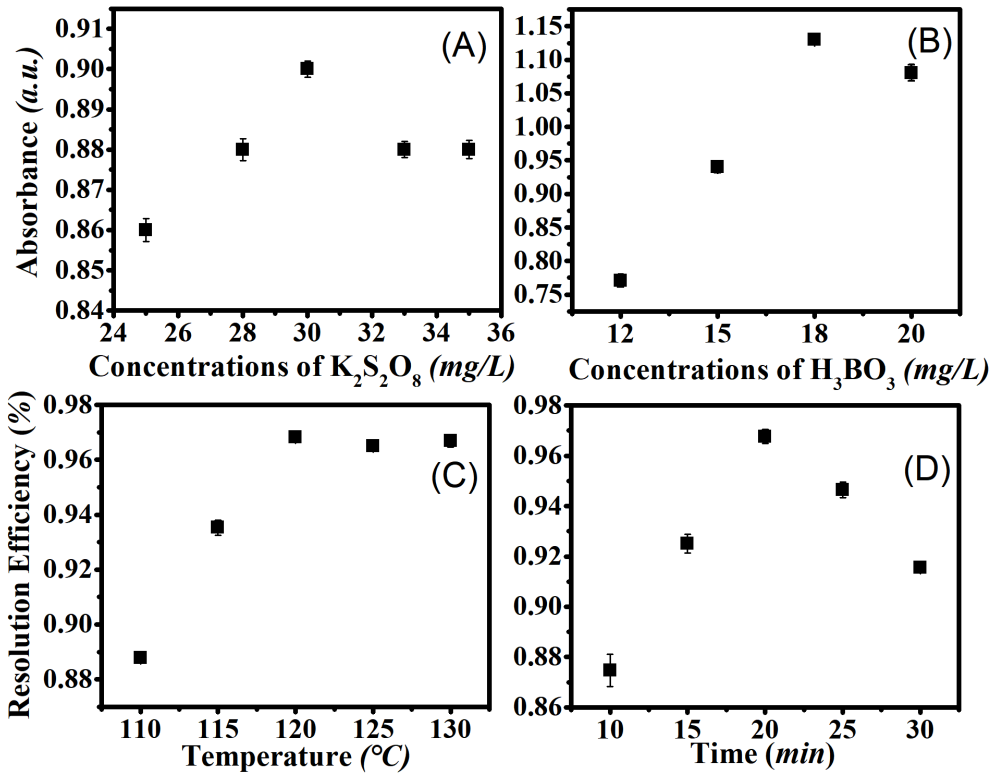

FIGURE 3
Optimization of digestion reaction conditions. 1.00 mg/L sodium β-glycerophosphate solution (calculated by P) was used to analyze the oxidation effect under oxidizer concentrations and varied reaction environment. **(A)** Optimization of oxidant concentration; **(B)** Optimization of H_3BO_3 Concentration (30g/L $K_2S_2O_8$); **(C)** Absorbance values at different reaction temperatures; **(D)** Absorbance values at different reaction time.

ascorbic acid concentration in the optimal sodium molybdate mixture. The figure indicates that with 83 μL of ascorbic acid, the absorbance value peaked at 0.58. Further increases in the number of steps for ascorbic acid led to a decrease in absorbance values.

The detection of phosphate color is influenced by different models of detection pools. Two types of cuvettes were analyzed, and experiments revealed that Z-shaped cuvettes are more appropriate for flow injection analysis (Figure 4C).

Coloring time is a critical factor influencing detection sensitivity and limit of detection. The relationship between coloring time and absorbance value was investigated experimentally. The results (Figure 4D) showed that the absorbance value increased with coloring time of up to 2 min. At 2 min, the absorbance value reached its peak. Beyond 2 min, the absorbance value stabilized and plateaued. Consequently, the optimal coloring time is 2 min. Therefore, the detection cycle is within 30 minutes, and the throughput of the sensor is 2 samples per hour.

Figure 5 presents the determination results for five representative phosphorus compounds, each prepared at 5.0 mg P/L. The digestion efficiencies for the different phosphorus-containing substances were 96.8% ± 0.8%, 97.5% ± 0.7%, 96.0% ± 1.3%, 100.1% ± 0.4%, and 87.3% ± 0.6%, respectively. As with other digestion methods (Worsfold et al., 2005), phosphorus recovery was compound-specific. For the phosphorus compounds with a C–O–P bond (β-SGP), the recovery was neer 100%, akin to the values reported for autoclave digestion with alkaline persulfate (Maher et al., 2002). Phosphorus compounds with a P–O–P bond (SHP, 5-PP) showed recoveries similar to those reported by Worsfold et al. (2005). However, the recovery for phosphorus compounds with a P–O–P bond (ATP) was 87.3% ± 0.6%, which was lower than the value reported by Huang and Zhang (2009), but close to the results obtained from autoclave persulfate digestion performed in this laboratory. The average recovery for the five compounds was 95.54% ± 0.76%, comparable to previous results from either acidic or alkaline persulfate autoclave methods, with no apparent correlation between recovery and compound structure (Huang and Zhang, 2008).

3.2 Sensor performance

The performance of the sensor was evaluated based on accuracy, precision, blank recovery, and sample recovery. The regression equation of TP in DI water was Y = 5806.80 X - 259.72, with R2 = 0.9996; where Y is the TP concentration and X is the absorbance (Figure 6A). The regression equation of TP in artificial seawater was Y = 498.87 X - 9.37, with R2 = 0.9995; where Y is the TP concentration and X is the absorbance (Figure 6B). The findings indicated that the detection limit for seawater samples was 1.9 μg/L, with a detection range of 6.5–1000 μg/L. For fresh water samples,

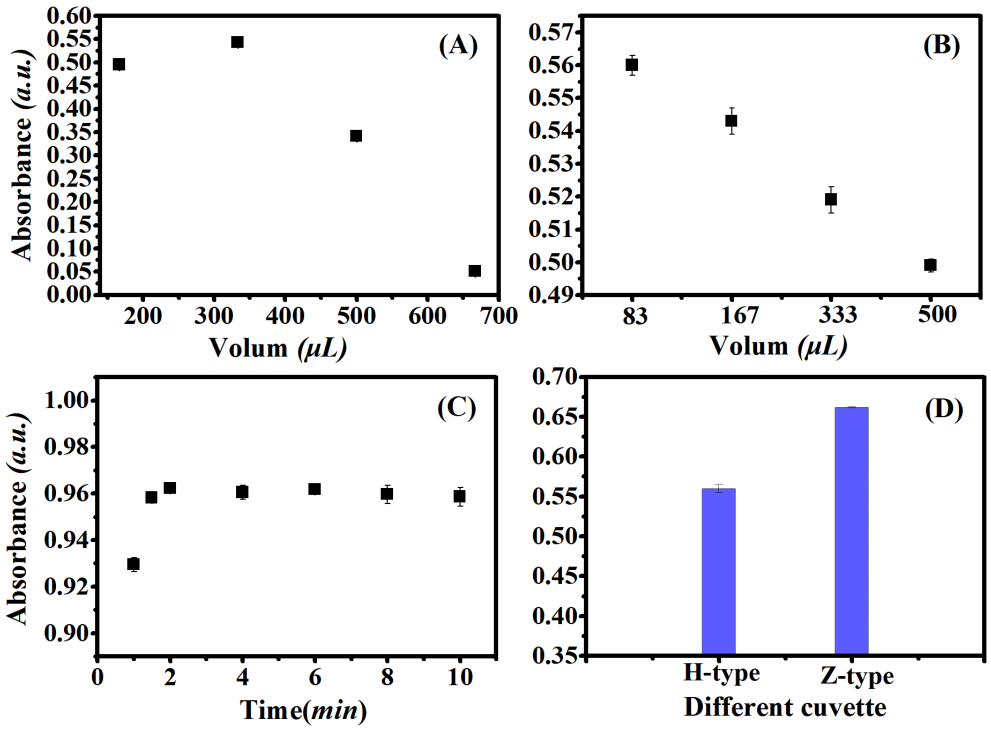

FIGURE 4
Different conditions for color reaction. Taking 1.00 mg/L sodium β-glycerophosphate solution (calculated by P) as an example under the optimal oxidation conditions. **(A)** Optimization of molybdate solution concentration; **(B)** Optimization of ascorbic Acid Concentration; **(C)** Absorbance values of different flow cell shapes; **(D)** The relationship between color development time and absorbance value.

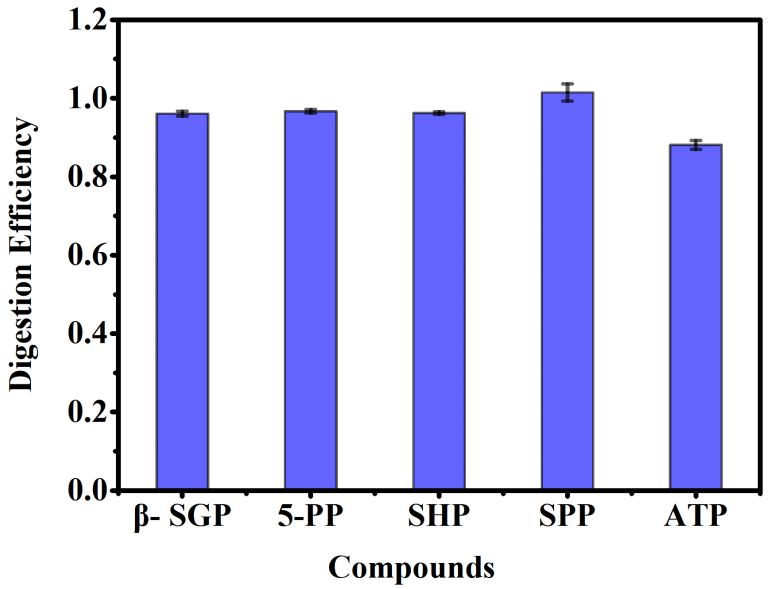

FIGURE 5
Digestion efficiency (%) of different phosphorus containing substances under the optimal reaction conditions. Samples were separately prepared at 5.0 mg P/L. β-Sodium glycerophosphate($C_3H_{12}NaO_7P$, β-SGP); 5-Pyridoxal phosphatemonohydrate ($C_8H_{10}NO_6P$, 5-PP); Sodium hexametaphosphate ($(NaPO_3)_6$, SHP); Sodium pyrophosphate($Na_4P_2O_7$, SPP); Adenosine 5'-triphosphate($C_{10}H_{16}N_5O_{13}P_3$, ATP).

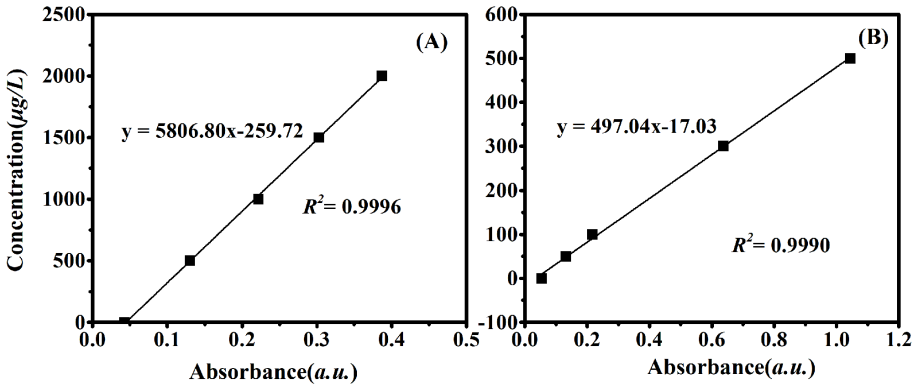

FIGURE 6
Standard curve of the sensor. The standard curve in pure aqueous solution was shown in **(A)**, which is suitable for monitoring fresh water from river water and tap water; **(B)** demonstrated the standard curve of artificial seawater for water quality monitoring in coastal waters.

such as river water, the detection limit was 1.2 μg/L, and the detection range was 4.1–2000 μg/L. The recovery rates for various water samples were assessed, and the test results are presented in Table 3. Recovery rates ranged from 97.59% to 103.19%.

Table 4 compares the flow methods or instrumental techniques for Phosphorus determination in water. Although some literature has lower detection limits than this article, underwater *in-situ* detection has not been achieved. There are other methods with a detection limit below 1 μg/L, but the detection parameter is phosphate, not total phosphorus. In contrast, the present method have achieved an *in-situ* monitoring of total phosphorus underwater with low detection limit.

3.3 Turbidity and temperature compensation algorithm

With small salinity variation in open seawater and the use of standard solutions of similar salinity to prepare standard curves,

TABLE 3 Sample recovery.

Sample	Salinity	Concentration (mg/L)	Added (mg/L)	Found (mg/L)	Recovery (%)
Standard solution	0	0.500	/	0.4978	99.56
		0.700		0.7474	106.77
		1.000		1.031	103.10
		1.500		1.5498	103.32
		2.000		1.9890	99.45
Standard solution	35	0.020	/	0.0185	92.50
		0.050		0.0488	97.60
		0.100		0.1010	101.00
		0.200		0.2104	105.20
		0.400		0.3802	95.05
		0.600		0.5990	99.83
		0.800		0.7960	99.50
		1.000		0.9688	96.88
Seawater 1	33	0.0318	0.200	0.2353	101.51
Seawater 2	33	0.0292	0.200	0.2287	99.78
Seawater 3	33	0.0287	0.200	0.2360	103.19
River	0	0.6234	0.200	0.8036	97.59

TABLE 4 Flow analysis methods for phosphorus determination in water.

Year	Title	Flow mode	Underwater measurements	Detected species	Detection Range/ Limite Of Detection	Matrix	Method description	References NO.	Ref.
2017	A Lab-On-Chip Phosphate Analyzer for Long-term *In Situ* Monitoring at Fixed Observatories: Optimization and Performance Evaluation in Estuarine and Oligotrophic Coastal Waters	Lab-on-chip	Yes	Phosphate	0.3-13 μmol/L	Water	describe the optimization of the molybdenum blue method for *in situ* work using a lab-on-chip (LOC) analyzer and evaluate its performance in the laboratory and at two contrasting field sites	39	Grand et al., 2017
2019	Realistic Measurement Uncertainties for Marine Macronutrient Measurements Conducted Using Gas Segmented Flow and Lab-on-Chip Techniques	SFA	NO	Phosphate	0.1 μmol/L	Marine	combine the routine analyses of certified reference materials (CRMs) with the application of a simple statistical technique to quantify the combined (random + systematic) measurement uncertainty associated with marine macronutrient measurements using gas segmented flow techniques	54	Birchill et al., 2019
2020	Development of an *In Situ* Analyzer Based on Sequential Injection Analysis and Liquid Waveguide Capillary Flow Cell for the Determination of Dissolved Reactive Phosphorus in Natural Waters	SIA	NO	Dissolved Reactive Phosphorus	1.4 μg/L	Natural Waters	with a 10 cm liquid waveguide capillary flow cell and a 6.3 min time cost of detection and a consumption of 23 μL at most for each reagent	33	Yang et al., 2020
2020	Automated simultaneous determination of total dissolved nitrogen and phosphorus in seawater by persulfate oxidation method	SCF	NO	Total Dissolved Phosphate	0.04 μmol/L	seawater	an automated persulfate oxidation method for the simultaneous determination of total dissolved nitrogen (TDN) and total dissolved phosphorus (TDP) in seawater using a gas-segmented continuous flow analyzer	27	Yasui-Tamura et al., 2020
2020	Monitoring of Total Phosphorus in Koto River by Flow Injection Analysis	FIA	NO	TP	3 μg/L	in Koto River	determined total phosphorus in the Koto river using fow injection analysis (FIA)	5	Asano and Shiraishi, 2020
2020	Automated determination of dissolved reactive phosphorus at nanomolar to micromolar levels in natural waters using a portable flow analyzer	SIA	NO	Dissolved Reactive Phosphorus	0.11 μmol/L	Natural Waters	a fully automated integrated syringe pump-based environmental-water analyzer (iSEA), which uses a syringe pump and multiposition selection valve to overcome the drawbacks of the current batch and continuous flow analyzers	48	Deng et al., 2020
2021	Sequential injection-square wave voltammetric sensor for phosphate detection in freshwater using silanized multi-walled carbon nanotubes and gold nanoparticles	SIA	NO	Phosphate	0.3 μg/L	Lake and pool water	detection with a glassy carbon electrode, modified with silanized carbon nanotubes and Au nanoparticles	69	Wu et al., 2021
2021	Exploring Ocean Biogeochemistry Using a Lab-on-chip Phosphate Analyser on an Underwater Glider	FIA	Yes	Phosphate	0.03 μmol/L	Seawater	a significant step forward in autonomous underwater vehicle sensor capabilities and presents new capability to extend research into the marine phosphorous cycle the first report of	82	Birchill et al., 2021

(Continued)

10.3389/fmars.2024.1492115

10.3389/fmars.2024.1492115

TABLE 4 Continued

Year	Title	Flow mode	Underwater measurements	Detected species	Detection Range/ Limite Of Detection	Matrix	Method description	References NO.	Ref.
							in situ ocean phosphate measurements conducted using an AUV		
2021	Industry Partnership: Lab on Chip Chemical Sensor Technology for Ocean Observing	FIA	Yes	Phosphate	0.04 µmol/L	Seawater	a new product line able to make high accuracy measurements of a number of water chemistry parameters *in situ*: i.e., submerged in the environment including in the deep sea (to 6,000 m)	118	Mowlem et al., 2021
2022	An Automated Analyzer for The Simultaneous Determination of Silicate and Phosphate in Seawater	SIA	NO	Phosphate	0.05 µmol/L	Seawater	a portable automated analyzer for the simultaneous determination of silicate and phosphate in water samples with varying salinity	46	Fang et al., 2022
	Our study	SIA	Yes	TP	1.9 µg/L	Marine Water	independent development of a sensor featuring an automated *in situ* detection technique. Utilizing potassium persulfate high-temperature oxidation and phosphorus molybdenum blue spectrophotometry, total phosphorus was monitored *in situ* via sequential injection technology	64	

salinity affected the total P detection. As well all know, silicic acid and arsenate are the main interfering ions of phosphate detection by the PMB method, because they can form similar blue compounds with molybdate to enhance the detection signal. However, it was found that the absorbance was unaffected by silicon concentrations below 100 µmol/L and arsenic below 150 nmol/L (Patey et al., 2010; Chen et al., 2021). In the oligotrophic open-ocean, silicon concentrations is lower than 2.5 µmol/L and arsenic concentrations is lower than 50 nmol/L (Patey et al., 2010; Wurl et al., 2013), thus the effect on the phosphate detection was negligible. In this paper, the sample was firstly filtered and converted into phosphate after high temperature and high pressure digestion for the detection of the total phosphorus concentration. The so-called interfering ions in the sample were oxidized during digestion, which had no effect on the subsequent detection.

The turbidity of samples can interfere with total phosphorus detection due to the presence of microorganisms, sediment, and other contaminants in water samples from real monitoring environments. To mitigate this interference, the reagent compensation method outlined in the national standard was employed. For flow injection analysis, prolonged measurement times and high turbidity in the developed color solution can lead to unstable measurement results. Therefore, in this study, a bucket filter of 10 µm without incrustation (Millipore, United States) was installed at the injection site to minimize sediment and other pollutants. At the same time, we measured the absorbance of the sample filtered by 10 µm to perform turbidity compensation. The absorbance value of the sample is the difference between the absorbance value after color development and the absorbance value of the filtered sample.

To better understand the trend of total phosphorus detection in water environments, temperature control of the sensor hardware and the environmental temperature compensation algorithm were implemented to eliminate temperature effects on detection. Specifically, the sensor was placed in a water bath to ensure that other boundary conditions remained constant except temperature (Figure 7). By varying the water bath temperature, a series of absorbance values were collected for the total phosphorus standard solution. Partial least squares model (PLS), as a powerful statistical modelling method is particularly suitable for detecting water quality parameters in modeling. The core of PLS is to handle the complex relationship between independent variables (temperature and absorbance) and dependent variables (TP concentration), which can be used to extract latent variables from the variables and address potential multicollinearity issues between independent variables (Cao et al., 2024).

In this work, the PLS was developed to predict values, where temperature and absorbance were used as input parameters with concentration as the output value. According to the control variable method, eight different temperatures (5, 10, 15, 20, 25, 30, 35, 40°C) and four different concentrations of TP (0, 50, 100, 200 µg/L) were set to measure output absorbance of the sensor that corresponded to different TP concentration values at different sets of temperatures and concentrations to obtain a series of data. The PLS method was used to construct the model. The advantage of this method is to

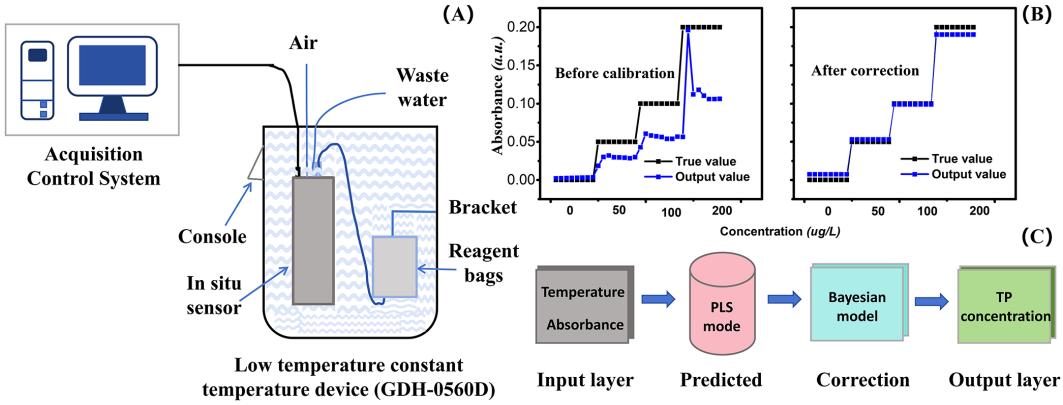

FIGURE 7
Temperature correction experimental device and schematic diagram. **(A)** is the schematic diagram of the experimental setup. Reagent bags content all liquid bags, including DI water, samples, standard solutions, oxidants, MS, and VC. **(B)** is the experimental result chart before and after Bayesian correction. The horizontal axis represents sample concentration, and the vertical axis represents absorbance. The black line represents the true value of the sample, and the blue line represents the output value after passing through the PLS model. **(C)** is the schematic diagram of temperature correction.

handle multicollinearity between independent variables, even if the number of variables is much larger than the sample size, it can still perform stable modeling. After the PLS calculation, the correlation coefficient between the prediction result and the real value is 0.8351.

Bayes' theorem can be widely applied in data analysis, pattern recognition, statistical decision-making, and the most popular artificial intelligence. In our study, the fitting degree of the corrected data improved from 0.8351 to 0.9926 compared to the precorrected data after the Bayesian correction model was applied for data compensation. The corrected data provides a more accurate representation of the total phosphorus content in the water quality at the monitoring site.

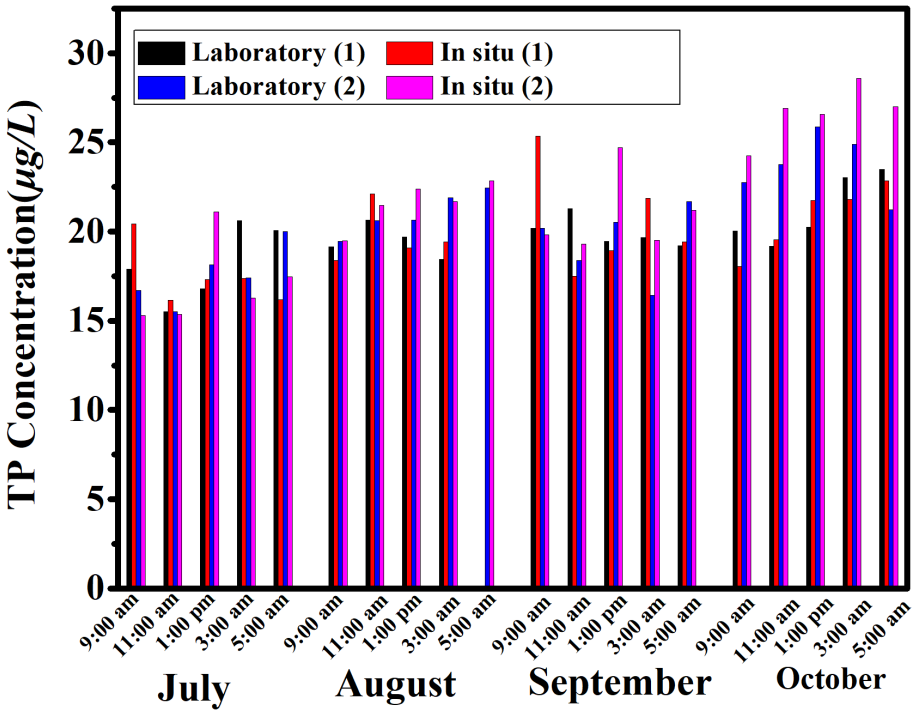

FIGURE 8
Comparison of laboratory test results and *in-situ* monitoring data. It represents laboratory testing data and sensor *in-situ* monitoring data from different time periods during the comparison period from July to October. Laboratory (1) represents the laboratory test results after collecting samples at various time periods on the first day of each month's comparison period; Laboratory (2) represents the laboratory test results after collecting samples at various time periods on the second day of the monthly comparison period; *In situ* (1) represents the monitoring data of sensors at various time periods on the first day of the monthly comparison period; *In situ* (2) represents the monitoring data of sensors at various time periods on the first day of the monthly comparison period. To reduce errors, the sampling time is kept consistent with the sensor injection time.

3.4 *In-situ* and online experiments

From July to October 2020, experiments were conducted over a four-month period. The *in situ* sensor was deployed on the barge at the Qingdao wharf, operating five times daily. Due to limitations in reagent validity and quantity, the sample was transported back to the laboratory for maintenance on a monthly basis. During this time, seawater samples were collected near the sensor on two days each month for laboratory analysis by the professional water sampler, with the data compared to the equipment's testing results (Figure 8). The concentration of total phosphorus in seawater remained relatively stable, varying between 15.31 and 28.59 μg/L. A minor increase in total phosphorus concentration was observed from July to October.

Additionally, the sensor was used at a river monitoring station in Zhejiang. During this period, construction work upstream caused the river water to become red and resulted in an increase in total phosphorus concentration. The on-site measurement of total phosphorus was 678.3 μg/L.

4 Conclusion

A portable analytical sensor has been effectively developed for *in situ* monitoring of total phosphorus concentrations in water. The sensor system includes an injection pump, digestion tubes for total phosphorus wet chemical reactions, and optical detection tanks for colorimetric analysis. The TP *in situ* sensor utilizes potassium persulfate high-temperature oxidation coupled with PMB spectrophotometry. A series of experiments were conducted to refine assay protocols and reaction conditions, validate the temperature compensation algorithm, and confirm the technical feasibility and reliability of the method. This sensor provides automation, minimizes manual labor, reduces reagent usage, and offers advantages such as rapid processing, low cost, and portability. It is suitable for analyzing river water, surface water, and industrial wastewater. Moreover, this autonomous *in situ* sensor can be utilized on both mobile and fixed platforms, including shore base stations, ships, and buoys.

Data availability statement

The raw data supporting the conclusions of this article will be made available by the authors, without undue reservation.

Author contributions

YMZ: Data curation, Methodology, Writing – original draft, Writing – review & editing. SC: Writing – review & editing. YL: Writing – review & editing. YZ: Data curation, Methodology, Writing – review & editing. YW: Investigation, Methodology, Writing – review & editing. SZ: Investigation, Writing – review & editing. XK: Supervision, Writing – review & editing. YG: Writing – review & editing. NG: Funding acquisition, Writing – review & editing.

Funding

The author(s) declare financial support was received for the research, authorship, and/or publication of this article. This work was supported by the National Natural Science Foundation of China (U2006209), the Science Education Industry Integration Pilot Major Innovation Project (2023HTZX01) of Qilu University of Technology (Shandong Academy of Sciences), the Natural Science Foundation of Shandong Province (No. ZR2019PD011, No. ZR2022QD013), and the National Natural Science Foundation of China (No. 42106185).

Acknowledgments

The authors would like to thank the Shiyanjia Lab (www.shiyanjia.com) for the language editing service.

Conflict of interest

The authors declare that the research was conducted in the absence of any commercial or financial relationships that could be construed as a potential conflict of interest.

Publisher's note

Supplementary material

The Supplementary Material for this article can be found online at: https://www.frontiersin.org/articles/10.3389/fmars.2024.1492115/full#supplementary-material

References

Alam, M., Srinivasan, V., Mueller, A., and Gu, A. (2021). Status and advances in technologies for phosphorus species detection and characterization in natural environment- a comprehensive review. *Talanta* 233, 122458. doi: 10.1016/j.talanta.2021.122458

Al-Shwaiyat, M., Vishnikin, A., Kharadzaha, A., and Bazel, Y. (2024). A non-extraction sequential injection method for determination ofloratadine using formation of its ion-association complex with bromocresolpurple in acetonitrile. *Talanta* 272, 125844. doi: 10.1016/j.talanta.2024.125844

Asano, H., and Shiraishi, Y. (2020). Monitoring of total phosphorus in Koto river by flow injection analysis. 3, 1-5. Available online at: https://www.researchgate.net/publication/340885177

Biocic, M., Kraljević, T., Spassov, T. G., Kukoc-Modun, L., and Kolev, S. D. (2024). Sequential injection analysis method for the determination of glutathione in pharmaceuticals. *Sensors* 24, 5677. doi: 10.3390/s24175677

Birchill, A. J., Beaton, A. D., Hull, T., Kaiser, J., Mowlem, M., Pascal, R., et al. (2021). Exploring ocean biogeochemistry using a lab-on-chip phosphate analyser on an underwater glider. *Front. Mar. Sci.* 8. doi: 10.3389/fmars.2021.698102

Birchill, A. J., Clinton-Bailey, G., Hanz, R., Mawji, E., Cariou, T., White, C., et al. (2019). Realistic measurement uncertainties for marine macronutrient measurements conducted using gas segmented flow and lab-on-chip techniques. *Talanta* 200, 228–235. doi: 10.1016/j.talanta.2019.03.032

Cao, Y., Zhu, J., Gao, Z., Li, S., Zhu, Q., Wang, H., et al. (2024). Spatial dynamics and risk assessment of phosphorus in the river sediment continuum (Qinhuai river basin, China). *Environ. Sci. pollut. Res.* 31, 2198–2213. doi: 10.1007/s11356-023-31241-w

Chen, L., Xu, J., Wang, T., Huang, Y., Yuan, D., and Gong, Z. (2021). Toward a versatile flow technique:Development and application of reverse flow dual-injection analysis (rFDIA) for determining dissolved iron redox species and soluble reactive phosphorus in seawater. *Talanta: Int. J. Pure Appl. Anal. Chem.* 232, 122404. doi: 10.1016/j.talanta.2021.122404

Dafner, E. V. (2016). An assessment of analytical performance of dissolved organic nitrogen and dissolved organic phosphorus analyses in marine environments: a review. *Int. J. Environ. Anal. Chem.* 96, 1188–1212. doi: 10.1080/03067319.2016.1246662

Deng, Y., Li, P., Fang, T., Jiang, Y., and Ma, J. (2020). Automated determination of dissolved reactive phosphorus at nanomolar to micromolar levels in natural waters using a portable flow analyzer. *Anal. Chem.* 92, 4379–4386. doi: 10.1021/acs.analchem.9b05252

Doyle, A., Weintraub, M. N., and Schimel, J. P. (2004). Persulfate digestion and simultaneous colorimetric analysis of carbon and nitrogen in soil extracts. *Soil Sci. Soc. America J.* 68, 669–676. doi: 10.2136/sssaj2004.6690

Fang, T. Y., Bo, G. Y., and Ma, J. (2022). An automated analyzer for the simultaneous determination of silicate and phosphate in seawater. *Talanta* 248, 123629. doi: 10.1016/j.talanta.2022.123629

Geißler, F., Achterberg, E. P., Beaton, A. D., Hopwood, M. J., Clarke, J. S., Mutzberg, A., et al. (2017). Evaluation of a ferrozine based autonomous *in situ* lab-on-chip analyzer for dissolved iron species in coastal waters. *Front. Mar. Sci.* 4. doi: 10.3389/fmars.2017.00322

Geißler, F., Achterberg, E. P., Beaton, A. D., Hopwood, M. J., Esposito, M., Mowlem, M. C., et al. (2021). Lab-on-chip analyser for the *in situ* determination of dissolved manganese in seawater. *Sci. Rep.* 11, 2382. doi: 10.1038/s41598-021-81779-3

Grand, M. M., Clinton-Bailey, G. S., Beaton, A. D., Schaap, A. M., Johengen, T. H., Tamburri, M. N., et al. (2017). A lab-on-chip phosphate analyzer for long-term *in situ* monitoring at fixed observatories: optimization and performance evaluation in estuarine and oligotrophic coastal waters. *Front. Mar. Sci.* 4. doi: 10.3389/fmars.2017.00255

Gray, H. E., Powell, T., Choi, S., Smith, D. S., and Parker, W. J. (2020). Organic phosphorus removal using an integrated advanced oxidation-ultrafiltration process. *Water Res.* 182, 115968. doi: 10.1016/j.watres.2020.115968

Huang, X. L., and Zhang, J. Z. (2008). Rate of phosphoantimonylmolybdenum blue complex formation in acidic persulfate digested sample matrix for total dissolved phosphorus determination: Importance of post-digestion pH adjustment. *Talanta* 77, 340–345. doi: 10.1016/j.talanta.2008.06.041

Huang, X. L., and Zhang, J. Z. (2009). Neutral persulfate digestion at sub-boiling temperature in an oven for total dissolved phosphorus determination in natural waters. *Talanta* 78, 1129–1135. doi: 10.1016/j.talanta.2009.01.029

Jia, Y., Sun, S., Wang, S., Yan, X., Qian, J., and Pan, B. (2023). Phosphorus in water: a review on the speciation analysis and species specific removal strategies. *Crit. Rev. Environ. Sci. technol.* 53, 435–456. doi: 10.1080/10643389.2022.2068362

Lei, Y., Saakes, M., Weijden, R.D.v. d., and Buisman, C. J. N. (2020). Electrochemically mediated calcium phosphate precipitation from phosphonates: Implications on phosphorus recovery from non-orthophosphate. *Water Res.* 169, 115206. doi: 10.1016/j.watres.2019.115206

Li, X., Liu, B., Ye, K., Ni, L., and Niu, X. (2019). Highly sensitive and specific colorimetric detection of phosphate by using zr(IV) to synergistically suppress the peroxidase-mimicking activity of hydrophilic fe3o4 nanocubes. *Sensors Actuators B: Chem.* 297, 126822. doi: 10.1016/j.snb.2019.126822

Lin, K. N., Ma, J., Yuan, D. X., Feng, S. C., Su, H. T., and Huang, Y. M. (2017). Sequential determination of multi-nutrient elements in natural water samples with a reverse flow injection system. *Talanta: Int. J. Pure Appl. Anal. Chem.* 167, 166–171. doi: 10.1016/j.talanta.2017.01.063

Lin, K. N., Xu, J., Guo, H. G., Huo, Y. L., and Zhang, Y. B. (2021). Flow injection analysis method for determination of total dissolved nitrogen in natural waters using on-line ultraviolet digestion and vanadium chloride reduction. *Microchem. Journal: Devoted to Appl. Microtech. all Branches Sci.* 164, 105993. doi: 10.1016/j.microc.2021.105993

Liu, C., Gao, S., Han, X., Tian, Y., Ma, J., Wang, W., et al. (2024). A violet light-emitting diode-based gas-phase molecular absorption device for measurement of nitrate and nitrite in environmental water. *Spectrochimica acta Part A. Mol. biomol. Spectrosc.*, 317, 124423. doi: 10.1016/j.saa.2024.124423

Liu, B., Su, H., Wang, S., Zhang, Z., Liang, Y., Yuan, D., et al. (2016). Automated determination of nitrite in aqueous samples with an improved integrated flow loop analyzer. *Sensors Actuators B Chem.* 237, 710–714. doi: 10.1016/j.snb.2016.07.002

MaChado, A., Marshall, G., Bordalo, A. A., and Mesquita, R. B. (2017). A greener alternative for inline nitrate reduction in the sequential injection determination of NO x in natural waters: replacement of cadmium reduction by UV radiation. *Anal. Methods* 9, 1876–1884. doi: 10.1039/C7AY00261K

Maher, W., Krikowa, F., Wruck, D., Louie, H., Nguyen, T., and Huang, W. Y. (2002). Determination of total phosphorus and nitrogen in turbid waters by oxidation with alkaline potassium peroxodisulfate and low pressure microwave digestion, autoclave heating or the use of closed vessels in a hot water bath: comparison with Kjeldahl digestion. *Analytica Chimica Acta*. 463, 283-293. doi: 10.1016/S0003-2670(02)00346-X

Mahmud, M., Ejeian, F., Azadi, S., Myers, M., and Asadnia, M. (2020). Recent progress in sensing nitrate, nitrite, phosphate, and ammonium in aquatic environment. *Chemosphere* 259, 127492. doi: 10.1016/j.chemosphere.2020.127492

Matzek, L. W., and Carter, K. E. (2016). Activated persulfate for organic chemical degradation: a review. *Chemosphere* 151, 178–188. doi: 10.1016/j.chemosphere.2016.02.05

Morgan, S., Luy, E., Furlong, A., and Sieben, V. (2021). A submersible phosphate analyzer for marine environments based on inlaid microfluidics. *Anal. Methods* 14, 22–33. doi: 10.1039/D1AY01876K

Mowlem, M., Beaton, A., Pascal, R., Schaap, A., Loucaides, S., Monk, S., et al. (2021). Industry partnership: lab on chip chemical sensor technology for ocean observing. *Front. Mar. Sci.* 8. doi: 10.3389/fmars.2021.697611

Nagul, E. A., Mckelvie, I. D., Worsfold, P., and Kolev, S. D. (2015). The molybdenum blue reaction for the determination of orthophosphate revisited: opening the black box. *Analytica Chimica Acta* 890, 60–82. doi: 10.1016/j.aca.2015.07.030

Nightingale, A. M., Beaton, A. D., and Mowlem, M. C. (2015). Trends in microfluidic systems for *in situ* chemical analysis of natural waters. *Sensors Actuators B: Chem.* 221, 1398–1405. doi: 10.1016/j.snb.2015.07.091

Patey, M. D., Achterberg, E. P., Rijkenberg, M. J. A., Statham, P. J., and Mowlem, M. (2010). Interferences in the analysis of nanomolar concentrations of nitrate and phosphate in oceanic waters, Anal. *Chim. Acta* 673, 109–116. doi: 10.1016/j.aca.2010.05.029

Perez de Vargas Sansalvador, I. M., Fay, C. D., Cleary, J., Nightingale, A. M., Mowlem, M. C., and Diamond, D. (2016). Autonomous reagent-based microfluidic PH sensor platform. *Sens. Actuators B 2016* 225, 369–376. doi: 10.1016/j.snb.2015.11.057

Peyton, G. R. (1993). The free-radical chemistry of persulfate-based total organic carbon analyzers. *Mar. Chem.* 41, 91–103. doi: 10.1016/0304-4203(93)90108-Z

Pinyorospathum, C., Rattanarat, P., Chaiyo, S., Siangproh, W., and Chailapakul, O. (2019). Colorimetric sensor for determination of phosphate ions using anti-aggregation of 2-mercaptoethanesulfonate-modified silver nanoplates and europium ions. *Sensors Actuators B: Chem.* 290, 226-232. doi: 10.1016/j.snb.2019.03.059

Rott, E., Minke, R., Bali, U., and Steinmetz, H. (2017). Removal of phosphonates from industrial wastewater with UV/FeII, Fenton and UV/Fenton treatment. *Water Res.* 122, 345–354. doi: 10.1016/j.watres.2017.06.009

Rusakov, A. V., Adamovich, B. V., Nurieva, N. I., Kovalevskaya, R. Z., Mikheyeva, T. M., Radchikova, N. P., et al. (2022). Phase synchronization of chlorophyll and total phosphorus oscillations as an indicator of the transformation of a lake ecosystem. *Sci. Rep.* 12, 11979. doi: 10.1038/s41598-022-16111-8

Ruzicka, J. J., and Chocholou, P. (2024). Next generation of flow analysis is based on flow programming. *Talanta* 269, 125410. doi: 10.1016/j.talanta.2023.12541

Salem, J. K., and Draz, M. A. (2020). Selective colorimetric nano-sensing solution for the determination of phosphate ion in drinking water samples. *Int. J. Environ. Anal. Chem.* 1-10. doi: 10.1080/03067319.2019.1702168

Shyla, B., Mahadevaiah,, and Nagendrappa, G. (2011). A simple spectrophotometric method for the determination of phosphate in soil, detergents, water, bone and food samples through the formation of phosphomolybdate complex followed by its reduction with thiourea. *Spectrochimica Acta Part A Mol. Biomol. Spectrosc.* 78, 497–502. doi: 10.1016/j.saa.2010.11.017

Sonnichsen, C., Atamanchuk, D., Hendricks, A., Morgan, S., Smith, J., Grundke, I., et al. (2023). An automated microfluidic analyzer for *in situ* monitoring of total alkalinity. *ACS Sens.* 2023, 8, 1, 344–352. doi: 10.1021/acssensors.2c02343

Sun, S., Shan, C., Yang, Z., Wang, S., and Pan, B. (2022). Self-enhanced selective oxidation of phosphonate into phosphate by Cu(II)/H2O2: Performance, mechanism, and validation. *Environ. Sci. Technol.* 56, 634–641. doi: 10.1021/acs.est.1c06471

Sun, S. H., Wang, S., Ye, Y. X., and Pan, B. C. (2019). Highly efficient removal of phosphonates from water by a combined Fe(III)/UV/co-precipitation process. *Water Res.* 153, 21–28. doi: 10.1016/j.watres.2019.01.007

Tambaru, D., Nagul, E. A., Almeida, M. I. G. S., and Kolev, S. D. (2024). Development of a sequential injection analysis method for the automatic speciation of inorganic selenium in water samples. *Microchem. J.* 201, 110688. doi: 10.1016/j.microc.2024.110688

Wang, J., and Wang, S. (2018). Activation of persulfate (PS) and peroxymonosulfate (PMS) and application for the degradation of emerging contaminants. *Chem. Eng. J.* 334, 1502–1517. doi: 10.1016/j.cej.2017.11.059

Worsfold, P. J., Clough, R., Lohan, M. C., Monbet, P., Ellis, P. S., Quétel, C. R., et al. (2013). Flow injection analysis as a tool for enhancing oceanographic nutrient measurements—A review. *Analytica Chimica Acta* 803, 15–40. doi: 10.1016/j.aca.2013.06.015

Worsfold, P. J., Gimbert, L. J., Mankasingh, U., Omaka, O. N., Hanrahan, G., Gardolinski, P. C. F. C., et al. (2005). Sampling, sample treatment and quality assurance issues for the determination of phosphorus species in natural waters and soils. *Talanta* 66, 273–293. doi: 10.1016/j.talanta.2004.09.006

Wu, T., Xia, D., Xu, J., Ye, C., Zhang, D., Deng, D., et al. (2021). Sequential injection-square wave voltammetric sensor for phosphate detection in freshwater using silanized multi-walled carbon nanotubes and gold nanoparticles. *Microchem. J.* 167, 106311. doi: 10.1016/j.microc.2021.106311

Wu, M., Zhang, T., Wan, D., and Xie, Y. (2022). Electrochemical impedance sensor based on nano-cobalt-oxide-modified graphenic electrode for total phosphorus determinations in water. *Int. J. Environ. Sci. Technol.* 19, 2635–2640. doi: 10.1007/s13762-021-03275-5

Wurl, O., Zimmer, L., and Cutter, G. A. (2013). Arsenic and phosphorus biogeochemistry in the ocean: arsenic species as proxies for P-limitation. *Limnol. Oceanogr.* 58, (2) 729–740. doi: 10.4319/lo.2013.58.2.0729

Yang, Z. M., Li, C., Lu, G. X., and Cao, W. (2019). A study of fast detection of nitrite in seawater based on sequential injection analysis. *Spectrosc. Spectr. Anal.* 39, 589–595. doi: 10.3964/j.issn.1000-0593(2019) 02-0589-07

Yang, Z., Li, C., Zhang, Z., Lu, G., Cai, Z., and Cao, W. (2020). Development of an *in situ* analyzer based on sequential injection analysis and liquid waveguide capillary flow cell for the determination of dissolved reactive phosphorus in natural waters. *Sensors (Basel Switzerland)* 20. doi: 10.3390/s20102967

Yang, S., Wang, P., Yang, X., Shan, L., Zhang, W., Shao, X., et al. (2010). Degradation efficiencies of azo dye acid orange 7 by the interaction of heat, uv and anions with common oxidants: persulfate, peroxymonosulfate and hydrogen peroxide. *J. Hazard. Mater.* 179, 552–558. doi: 10.1016/j.jhazmat.2010.03.039

Yasui-Tamura, S., Hashihama, F., Ogawa, H., Nishimura, T., and Kanda, J. (2020). Automated simultaneous determination of total dissolved nitrogen and phosphorus in seawater by persulfate oxidation method. *Talanta Open*. 2, 100016. doi: 10.1016/j.talo.2020.100016

Yin, T., Papadimitriou, S., Rérolle, V. M. C., Arundell, M., Cardwell, C. L., Walk, J., et al. (2021). A novel lab-on-chip spectrophotometric PH sensor for autonomous *in situ* seawater measurements to 6000 m depth on stationary and moving observing platforms. *Environ. Sci. Technol.* 55, 14968–14978. doi: 10.1021/acs.est.1c03517

Yokoyama, Y., Danno, T., Haginoya, M., Yaso, Y., and Sato, H. (2009). Simultaneous determination of silicate and phosphate in environmental waters using pre-column derivatization ion-pair liquid chromatography. *Talanta* 79, 308–313. doi: 10.1016/j.talanta.2009.03.053

Zhang, Y. M., Shi, Q., Sun, Z. L., Wang, Y., Zou, Y., Wang, Q., et al. (2019). Improvement of the uv-induced reduction efficiency of nitrate by manganese (ii) chloride based on sequential injection analysis. *IOP Conf. Series: Earth Environ. Sci.* 267, 032006. doi: 10.1088/1755-1315/267/3/032006

Zhang, Y. M., Zou, Y., Shi, Q., Wang, Y., Sun, Z. L., Wang, Q., et al. (2020). Determination of total dissolved nitrogen in seawater based on sequential injection analysis. *IOP Conference Series: Earth and Environmental Science* 461, 012017. doi: 10.1088/1755-1315/461/1/012017

Zhao, C., Chen, L., Zhong, G., Wu, Q., Liu, J., and Liu, X. (2021). A portable analytical system for rapid on-site determination of total nitrogen in water. *Water Res.* 202, 117410. doi: 10.1016/j.watres.2021.117410

Zhao, D., Liao, X., Yan, X., Huling, S. G., Chai, T., and Tao, H. (2013). Effect and mechanism of persulfate activated by different methods for pahs removal in soil. *J. Hazard. Mater.* 254–255, 228–235. doi: 10.1016/j.jhazmat.2013.03.056

Zhao, H. X., Liu, L. Q., Liu, Z. D., Wang, Y., Zhao, X. J., and Huang, C. Z. (2011). Highly selective detection of phosphate in very complicated matrixes with an off–on fluorescent probe of europium-adjusted carbon dots. *Chem. Commun.* 47, 2604–2606. doi: 10.1039/c0cc04399k

Zhu, J., Wang, S., Li, H., Qian, J., Lv, L., and Pan, B. (2021). Degradation of phosphonates in Co(II)/peroxymonosulfate process: Performance and mechanism. *Water Res.* 202, 117397. doi: 10.1016/j.watres.2021.117397